Refractive Intervention

Predicting Postoperative Anterior Chamber Angle for Phakic Intraocular Lens Implantation Using Preoperative Anterior Segment Metrics

Hannuy Choi[1,*], Taein Kim[2,*], Su Jeong Kim[2], Beom Gi Sa[2], Ik Hee Ryu[1,2], In Sik Lee[1], Jin Kuk Kim[1], Eoksoo Han[3], Hong Kyu Kim[4], and Tae Keun Yoo [1,2]

[1] Department of Refractive Surgery, B&VIIT Eye Center, Seoul, South Korea
[2] Research and Development Department, VISUWORKS, Seoul, South Korea
[3] Electronics and Telecommunications Research Institute (ETRI), Daejeon, South Korea
[4] Department of Ophthalmology, Dankook University Hospital, Dankook University College of Medicine, Cheonan, South Korea

Correspondence: Tae Keun Yoo, Department of Refractive Surgery, VISUWORKS, B&VIIT Eye Center, B2 GT Tower, 1317-23 Seocho-Dong, Seocho-Gu, Seoul, Republic of Korea. e-mail: eyetaekeunyoo@gmail.com

Purpose: The anterior chamber angle (ACA) is a critical factor in posterior chamber phakic intraocular lens (EVO Implantable Collamer Lens [ICL]) implantation. Herein, we predicted postoperative ACAs to select the optimal ICL size to reduce narrow ACA-related complications.

Methods: Regression models were constructed using pre-operative anterior segment optical coherence tomography metrics to predict postoperative ACAs, including trabecular-iris angles (TIAs) and scleral-spur angles (SSAs) at 500 μm and 750 μm from the scleral spur (TIA500, TIA750, SSA500, and SSA750). Data from three expert surgeons were assigned to the development ($N = 430$ eyes) and internal validation ($N = 108$ eyes) datasets. Additionally, data from a novice surgeon ($N = 42$ eyes) were used for external validation.

Results: Postoperative ACAs were highly predictable using the machine-learning (ML) technique (extreme gradient boosting regression [XGBoost]), with mean absolute errors (MAEs) of 4.42 degrees, 3.77 degrees, 5.25 degrees, and 4.30 degrees for TIA500, TIA750, SSA500, and SSA750, respectively, in internal validation. External validation also showed MAEs of 3.93 degrees, 3.86 degrees, 5.02 degrees, and 4.74 degrees for TIA500, TIA750, SSA500, and SSA750, respectively. Linear regression using the pre-operative anterior chamber depth, anterior chamber width, crystalline lens rise, TIA, and ICL size also exhibited good performance, with no significant difference compared with XGBoost in the validation sets.

Conclusions: We developed linear regression and ML models to predict postoperative ACAs for ICL surgery anterior segment metrics. These will prevent surgeons from overlooking the risks associated with the narrowing of the ACA.

Translational Relevance: Using the proposed algorithms, surgeons can consider the postoperative ACAs to increase surgical accuracy and safety.

Introduction

The implantation of posterior chamber phakic intraocular lens (IOL; EVO Implantable Collamer Lens [ICL]; STAAR Surgical, Lake Forest, CA, USA) has been widely performed to correct refractive errors.[1] Although the procedure is considered safe and effective,[2] angle closure and subsequent increase in intraocular pressure (IOP) may occur due to postoperative anatomic changes in the anterior chamber. In cases of severe complications, additional surgical procedures, such as ICL removal or exchange, can be indicated. Reduction of the anterior chamber angle (ACA) opening might be a critical condition—affecting aqueous humor flows—because the IOL
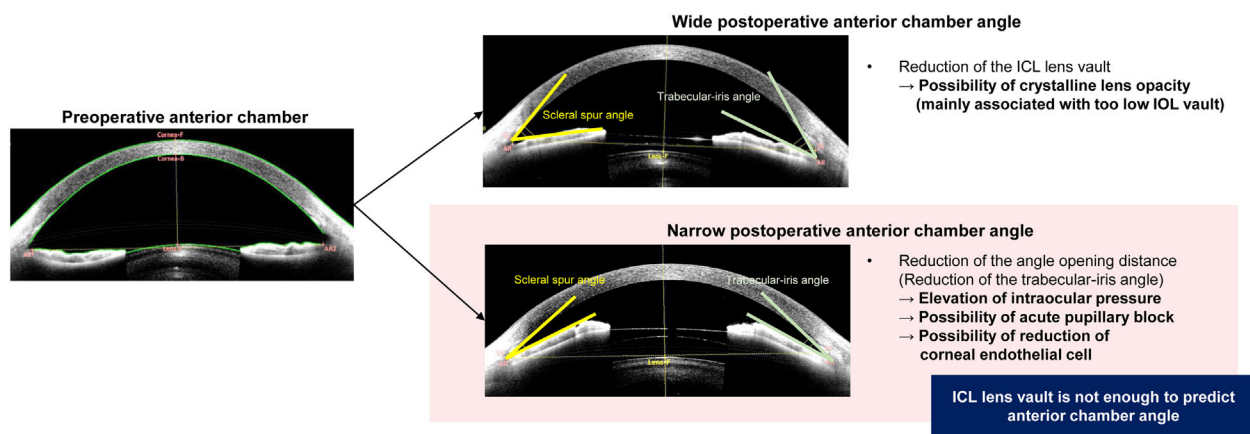
Figure 1. Schematic diagram of postoperative anterior chamber angle (ACA) changes and related complications after phakic intraocular lens implantation. Narrow ACAs including trabecular-iris angle (TIA) and scleral-spur angle (SSA) are associated with elevation of intraocular pressure and the possibility of acute pupillary block.

is located in the posterior chamber, lifting the iris into the anterior chamber.[3] In addition, a narrow ACA may affect the reduction of corneal endothelial cells.[4] Previously, studies have reported that a higher vault after implantation of ICL is associated with narrow ACA complications.[5] Because the size of the IOL is an important component in predicting postoperative ACA,[6] surgeons should carefully select the size to avoid complications by estimating the postoperative IOL vault in clinical practice.

Most previous studies have focused on postoperative IOL vaults following ICL surgery, but few have examined postoperative ACA changes.[6,7] A previous study reported that the pre-operative trabecular-iris angle (TIA) was the most important factor in predicting postoperative ACAs for ICL surgery.[8] However, considering postoperative TIA quantitively in clinics is limited because no study has developed postoperative ACA prediction models using biometric measurements. Recently, Nishida et al. established a postoperative TIA prediction model based on the predicted postoperative anterior chamber depth (ACD), pre-operative TIA, iris curvature, and iris space area.[9] However, this prediction model depended on the postoperative ACD prediction, which is the same as predicting the IOL vault, and it could not consider the effect of ICL size on the ACA.

Although the current consensus is that the postoperative IOL vault should range between 250 and 750 μm,[5,10] there is no agreement on postoperative ACAs such as TIA or scleral-spur angle (SSA). In our experience, large postoperative IOL vaults do not necessarily indicate a narrow ACA, and they are not a good predictor of postoperative ACA (Fig. 1). Aside from the IOL vault, a more precise postoperative prediction is required because better options may be available for selecting the size of the IOL, even within the appropriate vault range. Therefore, additional models predicting postoperative ACA are needed to achieve more accurate and safer ICL implantation. ACA prediction is critical for establishing the suitability of ICL implantation in patients with shallow ACD. Because machine-learning (ML) techniques have been used for vision correction surgeries,[11] we adopted them for more accurate outcome prediction.

Herein, we hypothesized that postoperative ACA changes are closely associated with the biometric factors of anterior segment optical coherence tomography (AS-OCT) and the size of the IOL, which is predictable. This retrospective study with a large dataset found a relationship between clinical measurements and postoperative ACA to identify significant factors for ACA prediction. To help clinicians predict postoperative TIAs and SSAs for selecting the optimal IOL size, we established and validated prediction models using statistical and ML approaches with AS-OCT and refractive features.

Methods

Data Collection

This study aimed to develop mathematical models to predict postoperative ACA values using pre-operative data. We retrospectively collected pre-operative and

postoperative ocular measurement data from the B&VIIT Eye Center (Seoul, South Korea). This study was approved by the institutional review board of the Korean National Institute for Bioethics Policy (No. P01-202208-01-037), and followed the tenets of the Declaration of Helsinki. From January to December 2021, the patients underwent vision correction surgery with posterior phakic intraocular lens implantation using an ICL (V5 models, EVO Visian ICL with KS-AquaPort). The inclusion criteria were: age 18 to 50 years, stable refraction, −0.50 to −20.00 diopters, hyperopia or myopia with astigmatism of ≤5.00 D, and availability of the preoperative AS-OCT measurements and the postoperative scanning results of AS-OCT for ACAs (TIA500, TIA750, SSA500, and SSA750) at 6 months postoperatively. AS-OCT was performed using CAISA2 (Tomey, Nagoya, Japan) under certain dark-light conditions using blackout curtains. To ensure a non-accommodative state, the patient was asked to stay at a far distance during all examinations. Patients with a history of ocular surgery, corneal disease, glaucoma, uveitis, or retinal disease were excluded from the study.

The selection of ICL size was based on the clinical decision obtained from the full evaluation by each surgeon. Before surgery, the surgeons decided on the lens size for each patient based on postoperative IOL vault predictions from the manufacturer's nomogram, KS-formula,[12] and AI-based method.[6] The surgeons decided the lens size for each patient based on postoperative IOL vault predictions, with a target size of 500 μm. All the surgeons were Korean board-certified ophthalmologists. Three expert surgeons had an average experience of 10 years, and one novice surgeon had 2 years of experience in ICL surgery. All operations were performed in a standard manner with a 3-mm clear corneal incision.[7]

Patients underwent pre-operative spherical equivalent (SE) measurements from manifest refraction, keratometry, pupil size (under dark conditions), and pre-operative white-to-white (WTW) distance measurements from Keratograph 4 (Oculus GmbH, Wetzlar, Germany). CASIA2 was done after 1 minute of dark adaptation.[6] One trained observer checked the scleral spur and angle points in each image during the examinations. The built-in 2D analysis program in CASIA2 allows the automatic calculation of measurements, structural outlines, and reference lines.[13] The image analysis process automatically measured central corneal thickness (CCT), angle-to-angle distance (ATA; the distance between 2 scleral spurs), According to the definitions, all factors were measured at 500 μm and 750 μm from the scleral spur or angle recessed lens, anterior chamber width (ACW; the distance between the 2 angle recesses), crystalline lens rise (CLR), and lens vault (LV). ACA-related factors, including angle opening distance (AOD), angle recess area (ARA), trabecular iris space area (TISA), and TIA were also automatically measured. At 6 months postoperatively, we measured ocular biometrics using CASIA2 and analyzed the data. Postoperative TIAs and SSAs were manually extracted from AS-OCT images through a retrospective chart review. All factors were measured at 500 and 750 μm from the scleral spur or angle recess according to the definitions (Supplementary Table S1).[8] For this analysis, we used the average value of the nasal and temporal measurements of TIA500, TIA750, SSA500, and SSA750.

We used anonymized medical records, pre-operative data, and 6-month postoperative data to develop and validate datasets. During the study, 538 eyes of 269 patients were operated on by 3 expert surgeons (training and internal validation), whereas 42 eyes of 21 patients were operated on by a novice surgeon (external validation). The training and internal validation datasets were obtained from three expert surgeons and randomly split. We assigned 430 eyes from 215 patients (80%) to the training dataset and 108 eyes from 54 patients (20%) to the internal validation dataset. A dataset from a novice surgeon was used to validate the model as an independent external dataset (42 eyes from 21 patients).

Model Development

We used statistical and ML models to predict the postoperative ACAs for ICL surgery, including TIA500, TIA750, SSA500, and SSA750. Furthermore, we constructed five postoperative ACA prediction models: (1) multivariable linear regression with variable selection (LR), (2) least absolute shrinkage and selection operator (LASSO), (3) support vector machine regressor with a Gaussian kernel (SVR), (4) random forest regression (RFR), and (5) extreme gradient boosting regression (XGBoost). LR and LASSO are the most popular methods for dimension reduction and robust linear regression in biomedical fields.[14] SVR is based on mapping data to a higher-dimensional space through a kernel function and choosing the best linear regressor that estimates training data.[15] RFR is an ensemble learning method, which consists of a collection of decision trees and can deal in training with high-dimensional data faster than other methods with a very robust performance.[16] XGBoost falls under larger parallel tree boosting

for regression and optimizes both the training loss and regularization of the model for the ensemble of the trees generated.[17] The codes and tutorials for XGBoost have been well documented in publicly available repositories (https://gist.github.com/pb111). The input variables for model development included age, sex, SE, mean keratometry, pupil size, IOP, WTW, CCT, ATA, ACD, ACW, CLR, LV, AOD500, AOD750, ARA500, ARA750, TISA500, TISA750, TIA500, TIA750, and ICL size.

Variable selection in the LR model was achieved by conducting both forward and backward stepwise selections. To avoid multicollinearity, we chose variables that were included in both stepwise selection processes. We also considered the variance inflation factor (VIF) to identify the independent predictors in the final regression model. The threshold value of VIF was set to >5, which means that the predictor was related to multicollinearity problems. Because VIF is an index representing the interactions between predictors (input factors), dependent variables (ACAs) are excluded from the VIF calculation by its definition. Generally, tree-based machine-learning techniques are known to have few multi-collinearity problems owing to their boosted nature,[18] therefore, we did not select variables for RFR and XGBoost.

To obtain an interpretation of the features from the XGBoost models predicting ACAs, we used the SHapley Additive exPlanations (SHAP) technique.[19] Presenting the SHAP feature importance in tree-based models is a standard approach.[20] The scikit-learn version 0.21.2 (Python library, https://scikit-learn.org/stable/) and RStudio version 3.5.1 (RStudio, Boston, MA, USA) were used to use the ML and SHAP algorithms. Additionally, the SHAP and XGBoost packages available in the GitHub repository (https://github.com/pablo14/shap-values) were used.

Pearson's correlation coefficients and mean absolute error (MAE) angles between the achieved and predicted ACA values were used to evaluate regression models. Data were analyzed using a linear mixed-effects model to provide more precise results while accounting for the inter-eye correlation.[21,22] To evaluate the predictive ability of the developed models for the risk of narrow postoperative ACAs (<20 degrees), we evaluated the postoperative TIA and SSA regression model results using receiver operating characteristic (ROC) curves, and calculated the areas under the curves (AUCs). Comparisons of the distribution of the datasets were performed using the chi-square test for categorical variables and the Student's *t*-test for continuous variables. The calculated MAEs were

compared using paired *t*-tests. All statistical analyses were conducted using RStudio statistical functions. Statistical tests were performed in a two-sided manner with a significance level of *P* value < 0.05.

Results

The patient demographics and ocular measurements are presented in Table 1. In total, 538 eyes from 274 patients who underwent surgery performed by 3e experienced surgeons were used for training (n = 430) and internal validation (n = 108). The dataset from a novice surgeon (42 eyes of 21 patients) was used for the external validation. All ICL surgeries were performed uneventfully, and no complications required additional surgical intervention. The distribution of the training dataset differed from that of the external validation datasets for pre-operative ACAs, including AOD, ARA, TISA, and TIA. None of the patients required an ICL size of 13.7 mm before surgery. The distribution of postoperative ACAs is shown in Supplementary Figure S1. In the training set, the pre-operative TIA500 and TIA750 were 57.4 degrees and 53.3 degrees, respectively, and the corresponding values decreased to 26.4 degrees and 26.0 degrees at 6 months postoperatively. Figure 2 shows the distribution of the actual postoperative ACAs compared to that of the postoperative IOL results using the entire dataset. No postoperative ACAs were correlated with postoperative IOL vault (Pearson correlation test: *P* value = 0.532 for TIA500, 0.123 for TIA750, 0.213 for SSA500, and 0.054 for SSA750). In our clinical observations, postoperative ACAs were independent conditions that were not affected by postoperative IOL vaults.

We explored the relationship between the pre-operative biometric variables and postoperative ACAs. Table 2 shows the correlation coefficients, univariate regression analyses, and VIFs. The pre-operative variables ACD, CLR, LV, AODs, ARAs, TISAs, and TIAs significantly correlated with postoperative TIAs and SSAs (*P* < 0.001). However, pre-operative ACAs revealed extremely high VIF values, indicating that they had a multi-collinearity problem. The ATA and ACW also had high VIF values of >10. It should be noted that the VIFs have the same value if there is the same combination of input variables.

Table 3 shows the multivariable LR analyses (linear mixed-effects models) for postoperative TIA values. The LR models with stepwise forward and backward selections identified pupil size, ATA, ACD, ACW, CLR, AOD500, TIA750, and ICL size as significant predictors of postoperative TIA500. However,

Table 1. Pre-Operative Demographics and Postoperative ICL Vaults of the Study Participants

	Training Dataset (3 Experts) (*N* = 430 Eyes from 215 Patients)	Internal Validation Dataset (3 Experts) (*N* = 108 Eyes from 54 Patients)	External Validation (One Novice) (*N* = 42 Eyes from 21 Patients)	P Value for Training Versus Internal Validation	P Value for Training Versus External Validation
Age, y	25.3 ± 6.1	25.5 ± 5.9	25.7 ± 6.6	0.869	0.688
Gender, female (*N* of patients, %)	130 (60.4)	34 (63.0)	13 (61.9)	0.666	0.941
Spherical equivalent (diopters)	−8.61 ± 2.28	−8.55 ± 2.24	−8.88 ± 1.98	0.822	0.406
Mean keratometry (diopters)	43.8 ± 1.4	44.0 ± 1.1	44.2 ± 1.3	0.112	0.095
Pupil size (under dark conditions, mm)	6.62 ± 0.68	6.58 ± 0.72	6.56 ± 0.54	0.614	0.547
Intraocular pressure (mm Hg)	14.8 ± 2.7	14.7 ± 2.6	14.7 ± 2.7	0.674	0.735
White-to-white (mm)	11.71 ± 0.36	11.67 ± 0.37	11.59 ± 0.39	0.370	0.073
Central corneal thickness (μm)	528.4 ± 36.1	531.1 ± 37.8	527.1 ± 32.6	0.496	0.822
Angle-to-angle distance (mm)	11.80 ± 0.37	11.75 ± 0.34	11.74 ± 0.46	0.203	0.395
Anterior chamber depth (mm)	3.36 ± 0.24	3.35 ± 0.25	3.31 ± 0.20	0.823	0.164
Anterior chamber width (mm)	11.84 ± 0.40	11.76 ± 0.36	11.78 ± 0.49	0.055	0.471
Crystalline lens rise (μm)	−77.0 ± 178.9	−77.2 ± 169.2	−63.3 ± 162.5	0.992	0.606
Lens vault (mm)	0.27 ± 0.16	0.28 ± 0.18	0.23 ± 0.16	0.690	0.098
AOD500 (mm)	0.77 ± 0.27	0.80 ± 0.32	0.67 ± 0.18	0.436	0.002
AOD750 (mm)	1.01 ± 0.31	1.05 ± 0.34	0.92 ± 0.22	0.339	0.015
ARA500 (mm^2)	0.28 ± 0.12	0.30 ± 0.14	0.24 ± 0.07	0.314	0.001
ARA750 (mm^2)	0.50 ± 0.18	0.52 ± 0.22	0.44 ± 0.12	0.355	0.006
TISA500 (mm^2)	0.26 ± 0.10	0.27 ± 0.12	0.22 ± 0.06	0.390	0.002
TISA750 (mm^2)	0.48 ± 0.17	0.50 ± 0.19	0.42 ± 0.11	0.368	0.007
TIA500 (degrees)	57.4 ± 13.1	57.3 ± 14.4	53.2 ± 9.0	0.964	0.007
TIA750 (degrees)	53.3 ± 11.4	53.6 ± 11.6	50.5 ± 7.8	0.803	0.037
Achieved ICL size				0.461	0.297
12.1 mm (*N* of eyes, %)	168 (39.1)	46 (42.6)	21 (50.0)		
12.6 mm (*N* of eyes, %)	228 (53.0)	57 (52.8)	17 (40.5)		
13.2 mm (*N* of eyes, %)	34 (7.9)	5 (4.6)	4 (9.5)		
Postoperative achieved ICL vault (μm)	536.5 ± 179.8	535.8 ± 156.9	502.7 ± 164.6	0.967	0.213
Postoperative TIA500 (degrees)	26.4 ± 7.0	25.4 ± 7.2	24.7 ± 5.9	0.207	0.086
Postoperative TIA750 (degrees)	26.0 ± 5.8	25.5 ± 6.1	24.3 ± 5.9	0.511	0.092
Postoperative SSA500 (degrees)	33.1 ± 8.2	32.1 ± 8.3	30.7 ± 8.1	0.278	0.084
Postoperative SSA750 (degrees)	30.6 ± 6.5	30.2 ± 6.8	28.8 ± 7.4	0.570	0.133

AOD500, angle open distance at 500 μm; AOD750, angle open distance at 750 μm; ARA500, angle recess area at 500 μm; ARA750, angle recess area at 750 μm; ICL, implantable collamer lens; SSA500, scleral spur angle at 500 μm; SSA750, scleral spur angle at 750 μm; TIA500, trabecular iris angle at 500 μm; TIA750, trabecular iris angle at 750 μm; TISA500, trabecular iris space area at 500 μm; TISA750, trabecular iris space area at 750 μm.

AOD500 was removed because it was not selected by both stepwise selection steps. ATA was also removed due to higher VIF (>5) to avoid a multicollinearity problem. Finally, pupil size, ACD, ACW, CLR, TIA750, and ICL size were selected for the final LR model to predict postoperative TIA500. In the prediction of postoperative TIA750, the same process was repeated and we obtained the same variables as the final predictors. The results of multivariable LR (linear mixed-effects models) for the postoperative SSA values
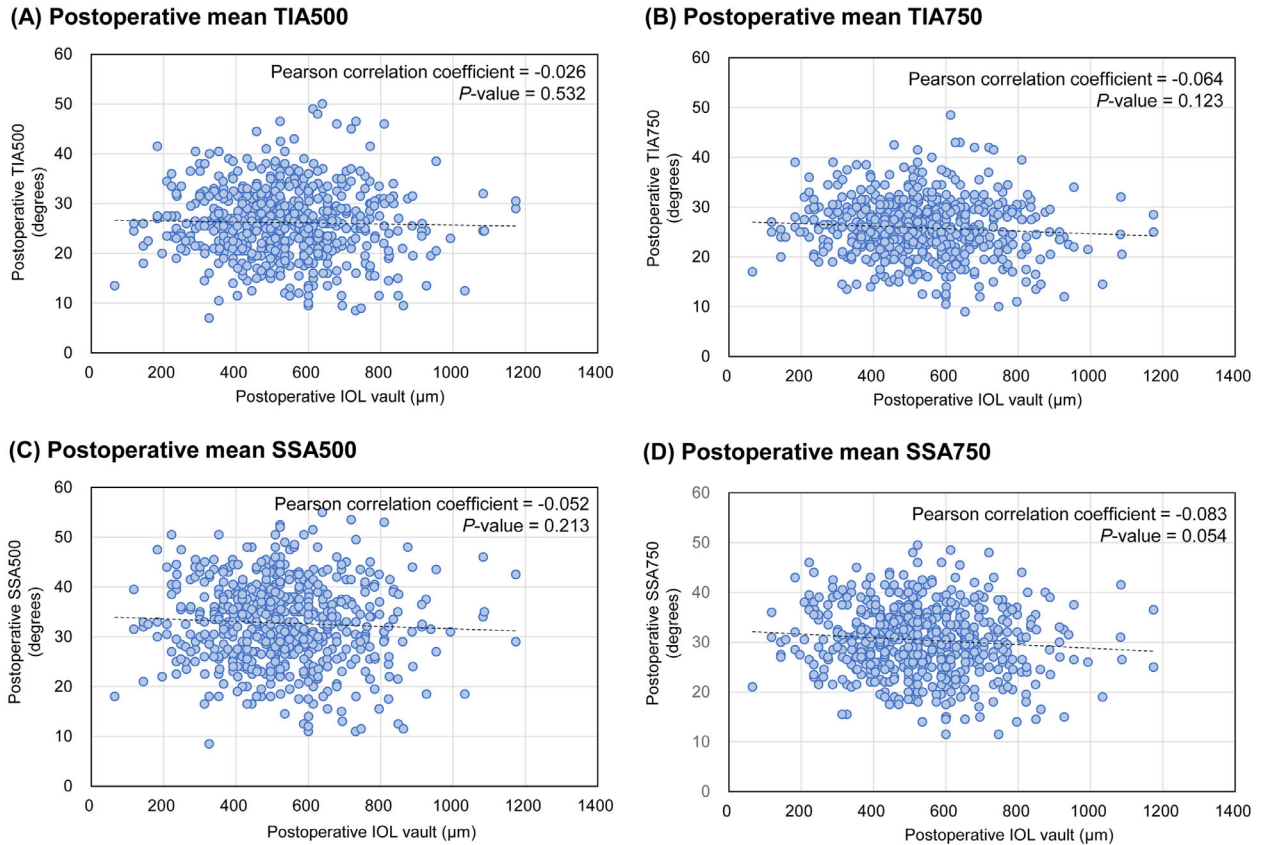
Figure 2. **The distribution of postoperative anterior chamber angles (ACAs) against postoperative vaults.** (**A**) The result of trabecular-iris angle at 500 μm (TIA500). (**B**) The result of trabecular-iris angle at 750 μm (TIA750). (**C**) The result of scleral-spur angle at 500 μm (SSA500). (**D**) The result of scleral-spur angle at 750 μm (TIA750). There are no significant correlations between ACAs and postoperative vaults.

are shown in Table 4. After stepwise variable selection and removal of the variables with higher VIF, the final LR models for postoperative SSAs also selected pupil size, ACD, ACW, CLR, TIA750, and ICL size as the final predictors. The variables in the final models showed low VIF values (<5). According to the results of the final LR models, equations were established to predict postoperative ACAs (Supplementary Table S2). The coefficients of ICL size for predicting postoperative ACAs showed significant negative values, indicating that implantation of a large ICL results in narrow postoperative ACAs. The data distribution and multivariable regression analysis showed that the ICL size interacted with ACD in predicting postoperative ACAs (Supplementary Fig. S2).

The SHAP technique estimated the feature importance of XGBoost models trained to predict postoperative ACAs (Fig. 3). The SHAP values showed that the ACD was the most critical predictor of postoperative ACAs. According to the model predicting postoperative TIA500, the top 5 important preoperative factors were ACD, TIA500, pupil size, TIA750, and ACW.

To predict TIA750, the top 5 factors were ACD, TIA750, pupil size, TIA500, and AOD750. According to the model predicting postoperative SSA500, the pre-operative variables of ACD, pupil size TISA500, TIA500, and CLR were the top 5 important factors. In the SSA750 model, the top 5 important pre-operative factors were ACD, TIA750, pupil size, CLR, and TISA500.

Scatter plots of the results comparing the actual and predicted ACAs are shown in Figure 4. In the internal validation, the Pearson correlation coefficients between the actual and predicted values of TIA500, TIA750, SSA500, and SSA750 were 0.636 ($P < 0.001$), 0.662 ($P < 0.001$), 0.630 ($P < 0.001$), and 0.659 ($P < 0.001$), respectively. The external validation showed correlation coefficients of 0.566 ($P < 0.001$), 0.627 ($P < 0.001$), 0.624 ($P < 0.001$), and 0.584 ($P < 0.001$) for TIA500, TIA750, SSA500, and SSA750, respectively. The overall MAEs achieved using the prediction methods for internal validation are listed in Table 5. XGBoost provided the lowest MAEs (4.42 degrees, 3.77 degrees, 5.25 degrees, and 4.30 degrees for TIA500,

translational vision science & technology

Table 2. Results of Univariate Linear Regression and Variance Inflation Factors for the Associations Between Pre-Operative Ocular Measurements and Postoperative Anterior Chamber Angles Using the Training Dataset

Pre-Operative Variables	Postoperative TIA500			Postoperative TIA750			Postoperative SSA500			Postoperative SSA750			
	Pearson Correlation Coefficient	Univariate Linear Regression β[a]	P Value	Pearson Correlation Coefficient	Univariate Linear Regression β[a]	P Value	Pearson Correlation Coefficient	Univariate Linear Regression β[a]	P Value	Pearson Correlation Coefficient	Univariate Linear Regression β[a]	P Value	VIF
Age, y	0.043	0.071	0.204	0.033	0.066	0.150	0.033	0.080	0.225	0.028	0.075	0.150	1.070
Gender, female	0.022	0.989	0.157	−0.049	−0.038	0.947	−0.021	−0.300	0.366	−0.090	−0.758	0.243	1.215
Spherical equivalent (diopters)	−0.006	−0.013	0.932	−0.013	−0.017	0.887	−0.005	−0.063	0.718	−0.029	−0.086	0.534	1.179
Mean keratometry (diopters)	0.118	0.682	0.006	0.149	0.679	0.001	0.083	0.549	0.061	0.121	0.596	0.010	2.943
Pupil size (under dark conditions, mm)	−0.166	−1.459	0.004	−0.165	−1.261	0.002	−0.156	−1.971	0.001	−0.146[b]	−1.524	0.001	1.212
Intraocular pressure (mm Hg)	−0.027	−0.027	0.828	−0.013	−0.008	0.936	0.001	0.113	0.437	0.012	0.098	0.396	1.562
White-to-white (mm)	0.110	1.881	0.042	0.102	1.317	0.083	0.089	1.212	0.265	0.089	1.012	0.240	4.128
Central corneal thickness (μm)	−0.042	−0.008	0.379	−0.039	−0.006	0.461	−0.008	−0.004	0.719	−0.005	−0.004	0.630	1.750
Angle-to-angle distance (mm)	0.019	0.341	0.708	0.012	0.007	0.993	0.082	1.509	0.158	0.071	0.950	0.261	12.842
Anterior chamber depth (mm)	0.429[b]	12.390	<0.001	0.465[b]	10.956	<0.001	0.426[b]	13.701	<0.001	0.467[b]	12.151	<0.001	7.441
Anterior chamber width (mm)	0.068	1.029	0.223	0.053	0.493	0.477	0.118	2.081	0.035	0.102	1.346	0.086	10.748
Crystalline lens rise (μm)	−0.185[b]	−0.007	<0.001	−0.218[b]	−0.007	<0.001	−0.148[b]	−0.007	0.002	−0.186[b]	−0.007	<0.001	4.932
Lens vault (mm)	0.261[b]	10.999	<0.001	0.290[b]	9.757	<0.001	0.263[b]	12.730	<0.001	0.288[b]	11.001	<0.001	4.509
AOD500 (mm)	0.428[b]	11.728	<0.001	0.450[b]	9.860	<0.001	0.401[b]	12.353	<0.001	0.429[b]	10.426	<0.001	77.380
AOD750 (mm)	0.413[b]	9.441	<0.001	0.440[b]	7.996	<0.001	0.399[b]	10.177	<0.001	0.431[b]	8.639	<0.001	44.198
ARA500 (mm²)	0.401[b]	24.728	<0.001	0.401[b]	19.693	<0.001	0.403[b]	27.939	<0.001	0.403[b]	21.939	<0.001	90.148
ARA750 (mm²)	0.412[b]	15.899	<0.001	0.411[b]	12.597	<0.001	0.416[b]	17.979	<0.001	0.417[b]	14.132	<0.001	182.126
TISA500 (mm²)	0.421[b]	30.457	<0.001	0.419[b]	24.212	<0.001	0.416[b]	34.094	<0.001	0.417[b]	26.903	<0.001	90.966
TISA750 (mm²)	0.428[b]	18.066	<0.001	0.426[b]	14.290	<0.001	0.424[b]	20.249	<0.001	0.428[b]	15.978	<0.001	128.133
TIA500 (degrees)	0.428[b]	0.240	<0.001	0.442[b]	0.200	<0.001	0.401[b]	0.258	<0.001	0.420[b]	0.214	<0.001	60.997
TIA750 (degrees)	0.399[b]	0.241	<0.001	0.417[b]	0.201	<0.001	0.392[b]	0.268	<0.001	0.413[b]	0.222	<0.001	78.547
ICL size (mm)	0.013	0.024	0.982	−0.009	−0.615	0.479	−0.009	−0.411	0.741	−0.023	0.229	0.816	3.617

AOD500, angle open distance at 500 μm; AOD750, angle open distance at 750 μm; ARA500, angle recess area at 500 μm; ARA750, angle recess area at 750 μm; ICL, implantable collamer lens; SSA500, scleral spur angle at 500 μm; SSA750, scleral spur angle at 750 μm; TISA500, trabecular iris space area at 500 μm; TISA750, trabecular iris space area at 750 μm; TIA500, trabecular iris angle at 500 μm; TIA750, trabecular iris angle at 750 μm; VIF, variance inflation factor.

[a] Regression coefficients of each univariate model.

[b] Correlation is significant with P value < 0.001.

Table 3. Results of Multivariable Linear Regression (Mixed Effect Model) for the Associations Between Pre-Operative Ocular Measurements and Postoperative Trabecular Iris Angles (TIAs) Using the Training Dataset

Target Variables	Pre-Operative Variables	Linear Regression with Stepwise Forward Selection				Linear Regression with Stepwise Backward Selection				Final Model[c]			
		β^a	Std β^c	P Value	VIF	β^a	Std β^c	P Value	VIF	β^a	Std β^b	P Value	VIF
Postoperative TIA500	Pupil size (under dark conditions, mm)	−2.258	−0.217	<0.001	1.134	−2.225	−0.214	<0.001	1.134	−2.308	−0.222	<0.001	1.128
	Angle-to-angle distance (mm)	−8.393	−0.445	<0.001	8.844	−6.059	−0.321	0.006	8.944	–	–	–	–
	Anterior chamber depth (mm)	11.835	0.407	<0.001	3.467	16.538	0.568	<0.001	2.870	15.818	0.544	<0.001	2.820
	Crystalline lens rise (μm)	0.009	0.237	<0.001	2.044	0.010	0.241	<0.001	2.044	0.009	0.221	<0.001	2.010
	Anterior chamber width (mm)	8.497	0.486	<0.001	8.207	5.276	0.302	0.006	7.432	1.221	0.070	0.032	3.012
	AOD500 (mm)	8.276	0.323	<0.001	2.378	–	–	–	–	–	–	–	–
	TIA750 (degrees)	0.059	0.095	0.068	1.799	0.129	0.210	<0.001	1.500	0.132	0.213	<0.001	1.499
	ICL size (mm)	−3.367	−0.154	0.029	3.283	−3.044	−0.139	0.056	3.278	−4.487	−0.205	0.003	2.921
Postoperative TIA750	Pupil size (under dark conditions, mm)	−1.847	−0.217	<0.001	1.134	−1.857	−0.218	<0.001	1.134	−1.927	−0.226	<0.001	1.128
	Angle-to-angle distance (mm)	−5.714	−0.369	0.001	9.016	−6.141	−0.397	0.001	9.303	–	–	–	–
	Anterior chamber depth (mm)	12.597	0.528	<0.001	3.497	12.542	0.525	<0.001	3.495	12.517	0.524	<0.001	2.820
	Crystalline lens rise (μm)	0.007	0.224	<0.001	2.061	0.007	0.215	<0.001	2.079	0.007	0.206	<0.001	2.010
	Anterior chamber width (mm)	5.679	0.396	<0.001	8.441	6.142	0.428	<0.001	8.890	1.651	0.115	0.098	3.012
	ARA500 (mm²)	–	–	–	–	9.887	0.208	<0.001	2.097	–	–	–	–
	TISA500 (mm²)	11.634	0.207	<0.001	2.218	–	–	–	–	–	–	–	–
	TIA750 (degrees)	0.056	0.110	0.030	1.742	0.059	0.116	0.021	1.696	0.065	0.129	0.012	1.499
	ICL size (mm)	−3.734	−0.208	0.003	3.279	−3.733	−0.208	0.003	3.279	−5.000	−0.278	<0.001	2.921

AOD500, angle open distance at 500 μm; AOD750, angle open distance at 750 μm; ARA500, angle recess area at 500 μm; ARA750, angle recess area at 750 μm; ICL, implantable collamer lens; SSA500, scleral spur angle at 500 μm; SSA750, scleral spur angle at 750 μm; TIA500, trabecular iris angle at 500 μm; TIA750, trabecular iris angle at 750 μm; TISA500, trabecular iris space area at 500 μm; TISA750, trabecular iris space area at 750 μm; VIF, variance inflation factor.

[a] Regression coefficients of the final regression model.

[b] Standardized regression coefficients of the final regression model.

[c] The model considering multi-collinearity and variable selection from the stepwise regression models.

translational vision science & technology

Table 4. Results of Correlation and Multivariable Linear Regression (Mixed Effect Model) With Stepwise Backward Selection Analysis for the Association Between Pre-Operative Ocular Measurements and Postoperative Scleral Spur Angles (SSAs) Using the Training Dataset

Target Variables	Pre-Operative Variables	Linear Regression with Stepwise Forward Selection				Linear Regression with Stepwise Backward Selection				Final Model[c]			
		β[a]	Std β[b]	P Value	VIF	β[a]	Std β[b]	P Value	VIF	β[a]	Std β[b]	P Value	VIF
Postoperative SSA500	Pupil size (under dark conditions, mm)	−2.894	−0.238	<0.001	1.134	−2.915	−0.239	<0.001	1.134	−3.007	−0.247	<0.001	1.128
	Angle-to-angle distance (mm)	−7.173	−0.324	0.006	9.016	−8.027	−0.363	0.003	9.303	—	—	—	—
	Anterior chamber depth (mm)	12.486	0.366	<0.001	3.497	12.370	0.362	<0.001	3.495	17.286	0.506	<0.001	2.820
	Crystalline lens rise (μm)	0.010	0.213	<0.001	2.061	0.009	0.202	<0.001	2.079	0.011	0.228	<0.001	2.010
	Anterior chamber width (mm)	10.085	0.492	<0.001	8.441	11.01	0.537	<0.001	8.890	3.348	0.163	0.021	3.012
	ARA500 (mm²)	—	—	—	—	19.683	0.290	<0.001	2.097	—	—	—	—
	TISA500 (mm²)	23.137	0.289	<0.001	2.180	—	—	—	—	—	—	—	—
	TIA750 (degrees)	0.090	0.124	0.018	1.742	0.095	0.132	0.023	1.696	0.161	0.222	<0.001	1.499
	ICL size (mm)	−5.497	−0.214	0.003	3.279	−5.496	−0.214	0.003	3.279	−6.303	−0.245	<0.001	2.921
Postoperative SSA750	Pupil size (under dark conditions, mm)	−2.337	−0.242	<0.001	1.134	−2.292	−0.238	<0.001	1.134	−2.349	−0.244	<0.001	1.128
	Angle-to-angle distance (mm)	−4.285	−0.245	0.032	8.844	−4.940	−0.282	0.017	9.303	—	—	—	—
	Anterior chamber depth (mm)	12.858	0.476	<0.001	3.467	13.081	0.484	<0.001	3.495	15.959	0.591	<0.001	2.820
	Crystalline lens rise (μm)	0.009	0.238	<0.001	2.044	0.008	0.212	0.004	2.079	0.008	0.231	<0.001	2.010
	Anterior chamber width (mm)	6.537	0.403	<0.001	8.207	7.125	0.439	<0.001	8.890	2.466	0.152	0.026	3.012
	AOD500 (mm)	6.000	0.252	<0.001	2.378	—	—	—	—	—	—	—	—
	ARA500 (mm²)	—	—	—	—	11.621	0.216	<0.001	2.097	—	—	—	—
	TIA750 (degrees)	0.060	0.104	0.043	1.799	0.073	0.128	0.011	1.696	0.112	0.195	<0.001	1.499
	ICL size (mm)	−5.590	−0.275	<0.001	3.283	−5.449	−0.268	<0.001	3.279	−5.973	−0.294	<0.001	2.921

AOD500, angle open distance at 500 μm; AOD750, angle open distance at 750 μm; ARA500, angle recess area at 500 μm; ARA750, angle recess area at 750 μm; ICL, implantable collamer lens; SSA500, scleral spur angle at 500 μm; SSA750, scleral spur angle at 750 μm; TIA500, trabecular iris angle at 500 μm; TIA750, trabecular iris angle at 750 μm; TISA500, trabecular iris space area at 500 μm; TISA750, trabecular iris space area at 750 μm.

[a]Regression coefficients of the final regression model.

[b]Standardized regression coefficients of the final regression model.

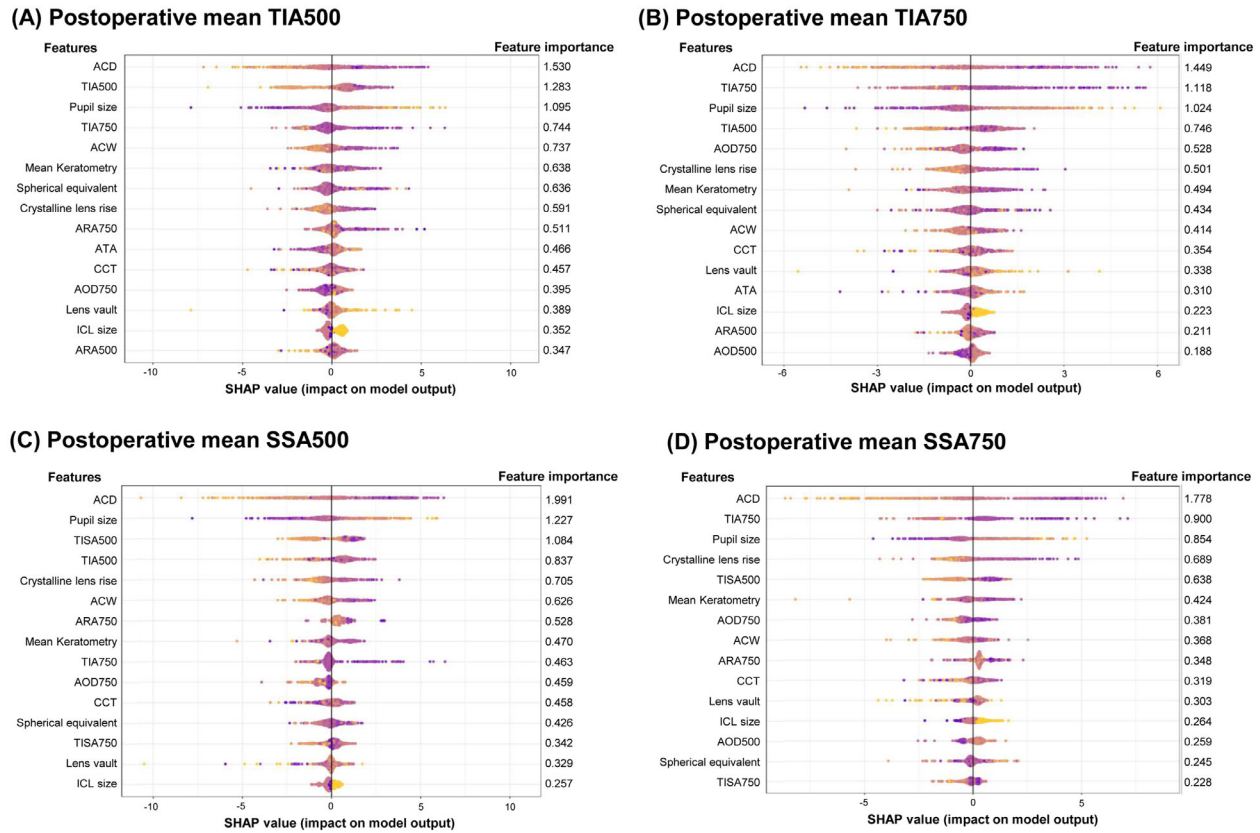[c]The model considering multi-collinearity and variable selection from the stepwise regression models.

Figure 3. The feature importance estimated by the SHAP technique using the proposed XGBoost model. The summary plots show the SHAP feature importance distributions. (**A**) The prediction result of trabecular-iris angle at 500 μm (TIA500). (**B**) The prediction result of trabecular-iris angle at 750 μm (TIA750). (**C**) The prediction result of scleral-spur angle at 500 μm (SSA500). (**D**) The prediction result of scleral-spur angle at 750 μm (TIA750).

TIA750, SSA500, and SSA750, respectively), but the differences were not significant compared with those obtained via the other methods for predicting all ACAs in the internal validation. As shown in Table 6, in the external validation, the LR model showed the lowest MAEs for TIAs (3.83 degrees and 3.71 degrees for TIA500 and TIA750, respectively) and SSAs (4.91 degrees and 4.70 degrees for SSA500 and SSA750, respectively); however, there were no significant differences compared with the other methods.

We attempted to detect narrow postoperative ACAs (<20 degrees) using the developed linear regression models (LR and XGBoost for continuous ACAs prediction). The ROC AUCs are shown in Figure 5. All prediction results showed good ROC AUCs of 0.79 or higher in the internal and external validation datasets. Five-fold cross-validation was performed owing to the small number of narrow ACA data, and similar results were obtained (Supplementary Fig. S3).

For a prompt hands-on experience with postoperative ACA prediction, we developed a simple web-based calculator application (https:

//taekeuntoo.github.io/) based on the final LR model using pupil size, ACD, ACW, CLR, TIA750, and ICL size, which was established in this study (Supplementary Fig. S4).

Discussion

We present statistical and ML approaches to predict postoperative ACA following ICL surgery, based on pre-operative biometric factors. Our proposed analysis successfully identified the significant factors associated with postoperative ACA changes, thus supporting our hypothesis that statistical and ML models can predict postoperative ACA. Furthermore, postoperative ACA was predictable based on a large retrospective analysis and postoperative IOL vault was not closely associated with postoperative ACA. The risk of ACA narrowing must also be determined with accurate prediction before ICL surgery. In the future, our algorithm will be useful for evaluat-
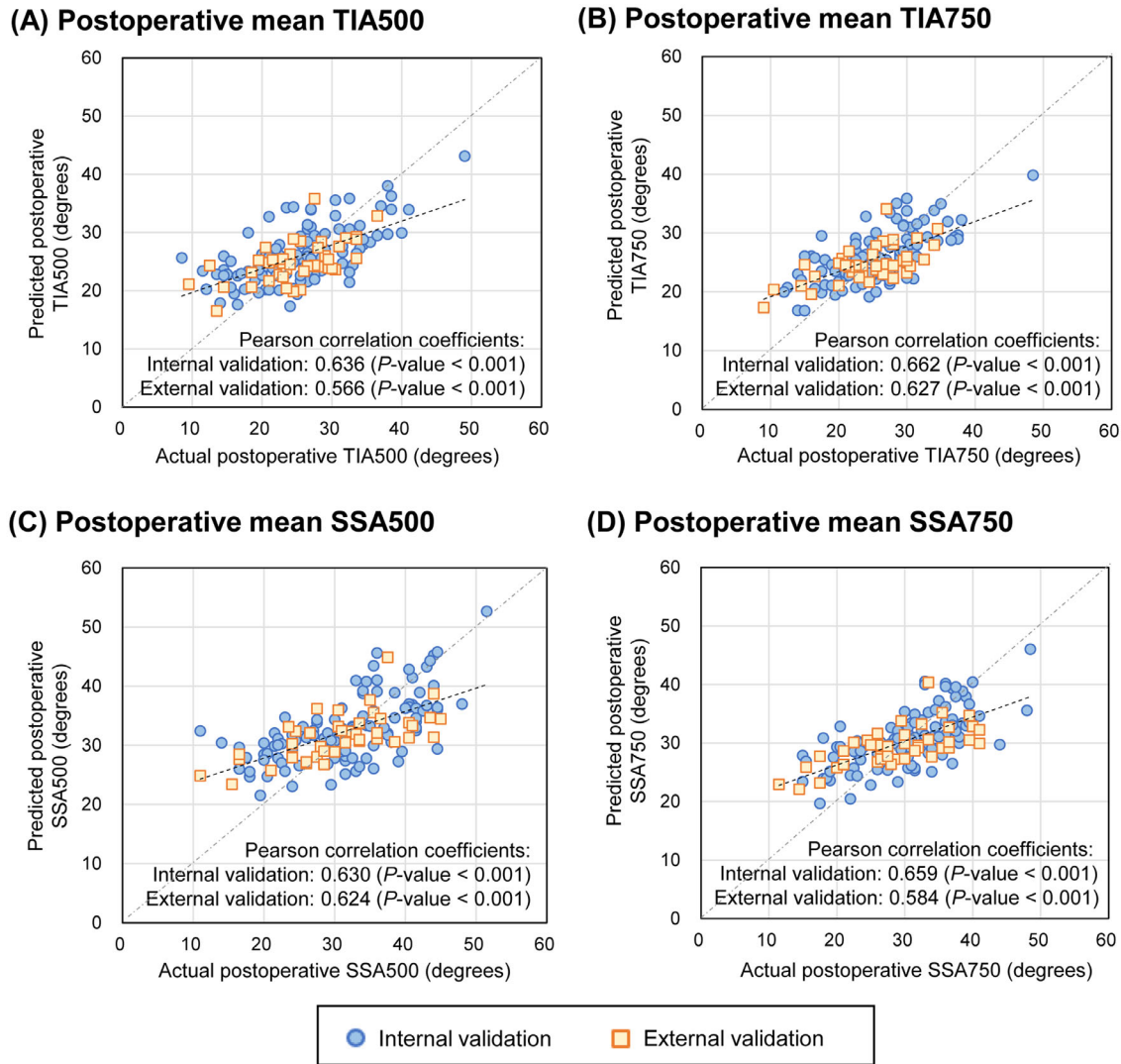
Figure 4. Performance of the developed machine-learning model to predict postoperative anterior chamber angles following ICL surgery. The plots show the distribution of the predicted anterior chamber angles against the actual postoperative results. (**A**) The prediction result of trabecular-iris angle at 500 μm (TIA500). (**B**) The prediction result of trabecular-iris angle at 750 μm (TIA750). (**C**) The prediction result of scleral-spur angle at 500 μm (SSA500). (**D**) The prediction result of scleral-spur angle at 750 μm (TIA750).

ing candidates for ICL surgery and selecting IOL size.

To our knowledge, this is the first ML model to predict comprehensive postoperative ACAs (TIA500, TIA750, SSA500, and SSA750) using pre-operative data. Several studies have reported a relationship between pre- and postoperative ACAs.[8,23,24] However, these studies included small datasets from <100 participants; moreover, no model was able to predict postoperative ACA. Nishida et al. established a postoperative TIA prediction model based on 174 eyes,[9] but their model was limited by its use of the predicted postoperative ACD without ICL size. Because Nishida et al. did not report the TIA measurement sites, its clinical applicability is limited. Our study

specifically predicted postoperative ACAs, including TIA500, TIA750, SSA500, and SSA750; therefore, our model could provide accurate structural prediction results.

Postoperative ACA prediction should be considered an essential issue in ICL surgery. Generally, phakic IOL implantation has been a safe option for vision correction in patients with a shallow anterior chamber or narrow ACA.[25] However, the long-term consequences of ACA narrowing have not been fully elucidated.[8] An observational study found that narrow ACA after ICL surgery may significantly influence the reduction of corneal endothelial cells.[4] Another study showed that approximately 15% of eyes with ICL surgery showed postoperative trabecular-iris contact.[8]

Table 5. Postoperative Anterior Chamber Angle Prediction Performance in the Internal Validation Dataset

Target Variables	Actual Angle (Achieved Angle)	LR	LASSO	SVR	RFR	XGBoost
Postoperative TIA500 (degrees)						
Prediction	25.28	26.30	25.97	25.96	25.97	25.93
SD	6.88	4.27	4.48	4.41	4.46	4.52
MAE	Reference	4.51	4.48	4.45	4.45	4.42
P value[a]	–	0.075	0.216	0.053	0.442	Reference
Postoperative TIA750 (degrees)						
Prediction	25.26	25.97	25.67	25.68	25.68	25.66
SD	6.10	3.80	3.79	3.79	3.84	3.98
MAE	Reference	3.83	3.78	3.84	3.83	3.77
P value[a]	–	0.802	0.845	0.308	0.170	Reference
Postoperative SSA500 (degrees)						
Prediction	31.72	32.83	32.50	32.49	32.51	32.45
SD	8.30	5.03	5.08	5.01	5.10	5.22
MAE	Reference	5.38	5.27	5.38	5.31	5.25
P value[a]	–	0.073	0.969	0.104	0.287	Reference
Postoperative SSA750 (degrees)						
Prediction	29.82	30.29	30.26	30.27	30.26	30.22
SD	7.04	4.08	4.20	4.01	4.23	4.41
MAE	Reference	4.38	4.33	4.44	4.33	4.30
P value[a]	–	0.196	0.592	0.262	0.568	Reference

LASSO, least absolute shrinkage and selection operator; LR, linear regression with backward stepwise selection; MAE, mean absolute error; RFR, random forest regressor; SSA500, scleral spur angle at 500 μm; SSA750, scleral spur angle at 750 μm; SVR, support vector regressor; TIA500, trabecular iris angle at 500 μm; TIA750, trabecular iris angle at 750 μm; XGBoost, extreme gradient boosting.

[a]Calculated using the difference between MAE values.

Because trabecular-iris contact means a block of aqueous humor flows, elevated IOP with angle closure or increased trabecular pigmentation can occur.[26] If this contact is not resolved, surgical interventions, such as iridectomy, lens exchange into a smaller size, or IOL removal, may be needed. Our study revealed that postoperative TIA and SSA were predictable (see Supplementary Fig. S2) and not associated with postoperative vaults, as shown in Figure 2. Therefore, both postoperative IOL vault and independent postoperative ACA prediction models are necessary to evaluate suitability and select the optimal IOL size for ICL surgery.

According to our observations, the common belief that high IOL vaults produce excessive narrowing of the ACA is not always clinically applicable (see Fig. 2). Postoperative vault is still a major parameter to consider for the suitability and determination of lens size. Too high a vault is associated with pupil abnormality and IOL dislocation, whereas too low a vault is associated with anterior subcapsular cataract formation.[27] In our prediction models, implantation of a large-size IOL resulted in a more narrow postoperative ACA. Therefore, surgeons should consider postoperative IOL vaults and ACAs to achieve safe and good surgical outcomes. Considering only the IOL vault while overlooking ACAs may result in ACAs that are postoperatively too narrow, as shown in the case examples in Figure 6. The cases show that both sizes of 12.1 mm and 12.6 mm were acceptable according to postoperative IOL vaults predicted by the KS formula and ML algorithm.[7] Although this analysis is based on a retrospective review, a smaller size might be a better option according to the ACA prediction results. Figure 7 shows that the proposed algorithms can also be useful when considering IOL exchange surgeries. Using the proposed calculation, it is possible to predict whether the ACA is stable after surgery. Our proposed method complements the conventional IOL size selection based on vault prediction and produces more accurate surgical outcomes.

The prediction performance was reduced in the external validation set collected by a novice surgeon. Although ICL surgery has been almost standardized,

Table 6. Postoperative Anterior Chamber Angle Prediction Performance in the External Validation Dataset

Target Variables	Actual Angle (Achieved Angle)	LR	LASSO	SVR	RFR	XGBoost
Postoperative TIA500 (degrees)						
Prediction	24.76	25.14	25.04	25.02	25.03	24.93
SD	5.92	3.29	3.50	3.46	3.48	3.56
MAE	Reference	3.83	3.91	3.89	3.92	3.93
P value	–	Reference	0.751	0.793	0.727	0.702
Postoperative TIA750 (degrees)						
Prediction	24.39	25.01	24.87	24.91	24.83	24.74
SD	5.90	2.85	2.98	2.98	2.99	3.06
MAE	Reference	3.71	3.83	3.87	3.86	3.86
P value	–	Reference	0.493	0.361	0.417	0.442
Postoperative SSA500 (degrees)						
Prediction	30.75	31.83	31.57	31.62	31.62	31.49
SD	8.16	3.78	4.02	3.79	3.83	4.02
MAE	Reference	4.91	4.99	5.02	4.97	5.02
P value	–	Reference	0.238	0.197	0.268	0.229
Postoperative SSA750 (degrees)						
Prediction	28.81	29.467	29.53	29.92	29.47	29.35
SD	7.46	3.21	3.26	3.23	3.27	3.39
MAE	Reference	4.70	4.76	4.79	4.73	4.74
P value	–	Reference	0.490	0.405	0.615	0.581

LASSO, least absolute shrinkage and selection operator; LR, linear regression with backward stepwise selection; SSA500, scleral spur angle at 500 µm; RFR, random forest regressor; SSA750, scleral spur angle at 750 µm; SVR, support vector regressor; TIA500, trabecular iris angle at 500 µm; TIA750, trabecular iris angle at 750 µm; XGBoost, extreme gradient boosting.
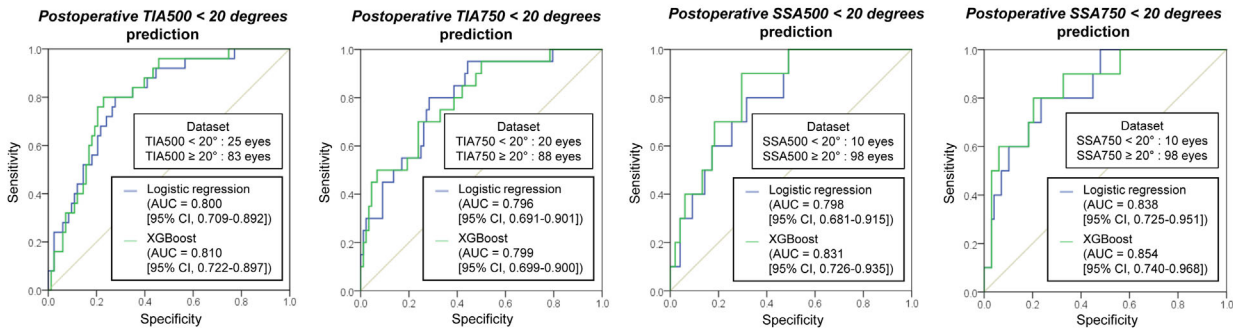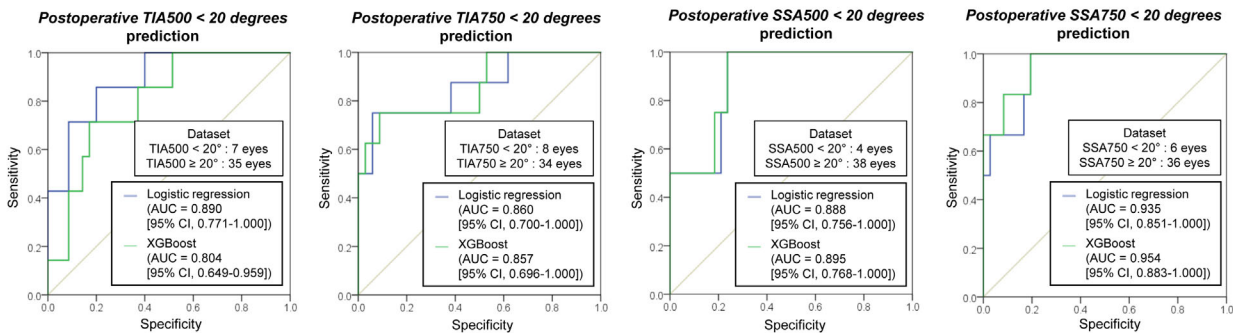

Figure 5. Classification performance of the developed models (linear regression models) to detect narrow postoperative anterior chamber angles (<20 degrees). (**A**) The prediction result from the internal and (**B**) external validation.
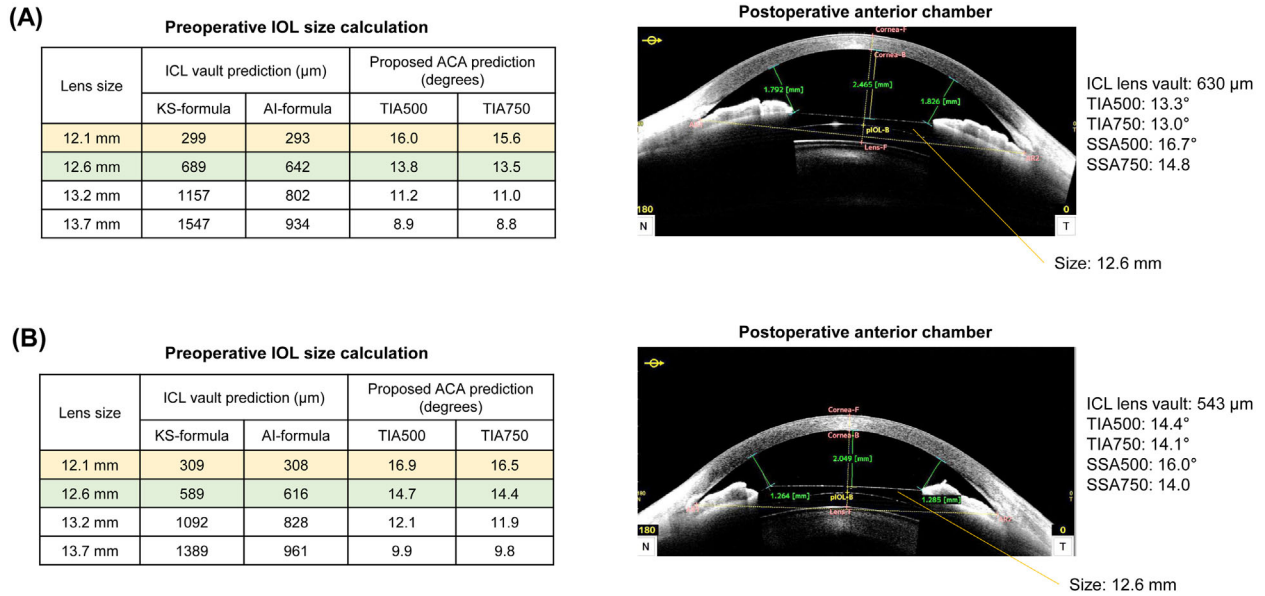
(A)

Preoperative IOL size calculation

Lens size	ICL vault prediction (μm)		Proposed ACA prediction (degrees)	
	KS-formula	AI-formula	TIA500	TIA750
12.1 mm	299	293	16.0	15.6
12.6 mm	689	642	13.8	13.5
13.2 mm	1157	802	11.2	11.0
13.7 mm	1547	934	8.9	8.8

Postoperative anterior chamber

ICL lens vault: 630 μm
TIA500: 13.3°
TIA750: 13.0°
SSA500: 16.7°
SSA750: 14.8

Size: 12.6 mm

(B)

Preoperative IOL size calculation

Lens size	ICL vault prediction (μm)		Proposed ACA prediction (degrees)	
	KS-formula	AI-formula	TIA500	TIA750
12.1 mm	309	308	16.9	16.5
12.6 mm	589	616	14.7	14.4
13.2 mm	1092	828	12.1	11.9
13.7 mm	1389	961	9.9	9.8

Postoperative anterior chamber

ICL lens vault: 543 μm
TIA500: 14.4°
TIA750: 14.1°
SSA500: 16.0°
SSA750: 14.0

Size: 12.6 mm

Figure 6. Examples of postoperative ICL vault, anterior chamber angle (ACA) prediction, and lens size selection cases using the proposed prediction model application. (**A**) A 31-year-old woman with narrow postoperative ACA. (**B**) A 27-year-old woman with narrow postoperative ACA. The ICL vaults are calculated using the KS-formula[12] and AI-based[6] methods.

(A)

IOL exchange

ICL size (mm)
12.6 → 13.2

ICL size: 12.6 mm
Actual TIA500 = 35.3°
Actual TIA750 = 32.5°
Proposed ACA prediction (TIA500) = 34.4°
Proposed ACA prediction (TIA750) = 33.9°

ICL size: 13.2 mm
Actual TIA500 = 30.9°
Actual TIA750 = 28.7°
Proposed ACA prediction (TIA500) = 31.4°
Proposed ACA prediction (TIA750) = 30.8°

(B)

IOL exchange

ICL size (mm)
13.2 → 12.6

ICL size: 13.2 mm
Actual TIA500 = 18.6°
Actual TIA750 = 16.5°
Proposed ACA prediction (TIA500) = 21.1°
Proposed ACA prediction (TIA750) = 20.6°

ICL size: 12.6 mm
Actual TIA500 = 27.9°
Actual TIA750 = 25.4°
Proposed ACA prediction (TIA500) = 24.0°
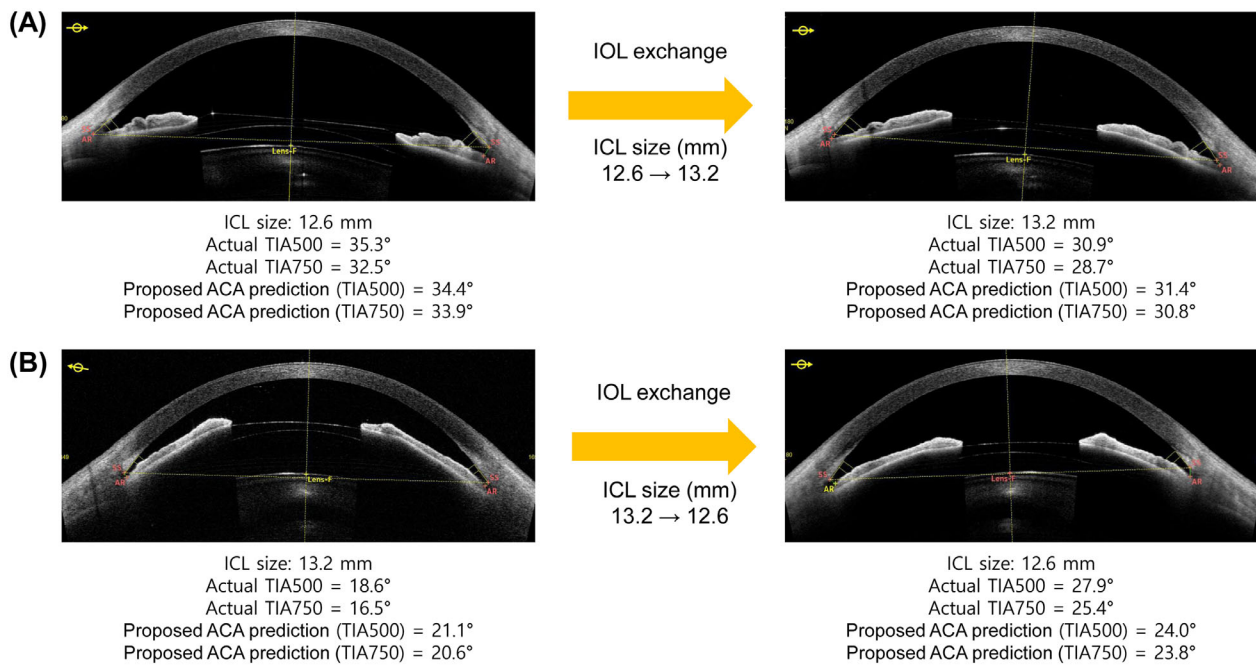Proposed ACA prediction (TIA750) = 23.8°

Figure 7. **Examples of postoperative anterior chamber angle changes in IOL exchange surgeries.** (**A**) A case in which the size of the ICL was changed to a larger one. (**B**) A case in which the size of the ICL was changed to a smaller one.

different surgical skills might have affected the clinical outcome in this study. Some ML studies have shown decreased performance in external validation. For example, the ICL vault prediction model trained with the Korean population showed lower predictive performance in the Japanese population.[6,7] A review on deep-learning algorithms summarized that many studies reported a performance decrease in external validation compared with that associated with internal validation.[28]

The SHAP description of XGBoost, which is based on boosting, shows relatively low importance of ICL

size because it extracts impacts of factors without considering multi-collinearity.[29] Therefore, variables with high VIFs, which were removed from the LR models, such as ATA, AOD, ARA, and TISA, received high SHAP importance scores. However, the ICL size is the only adjustable variable among the input factors in this analysis. Therefore, even if the ICL size exhibits relatively little importance in ML algorithms and regression equations, the clinical significance is the greatest in all prediction models. As observed in the IOL exchange cases (see Fig. 7), the change in ICL size actually significantly impacts the postoperative ACAs changes. Unlike the postoperative IOL vault, which was most affected by ICL size, the postoperative ACA was more influenced by anatomic factors than the ICL size. Most studies have demonstrated that postoperative vaults can be predicted using ICL size, ACD, ACW, CLR, or ATA.[6,30] According to the regression analysis in our study, pre-operative measurements, including pupil size, ACD, ACW, CLR, TIA, and ICL size, were significantly associated with postoperative ACAs. The ML analysis revealed similar results; ACD, TIA, and pupil size were the major factors affecting postoperative ACAs. This finding slightly disagrees with similar observations reported by a study that revealed that age, SE, and axial length were critical factors affecting postoperative ACA.[8] Our observation found that ocular anatomic measurements of the anterior segment without age, SE, and axial length could predict the postoperative ACA changes with a moderate correlation.

ML techniques did not significantly improve prediction performance compared to the LR and LASSO techniques in both internal and external validation. ML techniques demonstrably outperform high-dimensional complex datasets. The good performance obtained using only LR suggests that the interactions between biometric measurements are not complex regardless, of the underlying difficulty of the prediction task. In particular, the use of ML was not beneficial, with higher MAEs in external validation. Owing to the relatively small size of our dataset, overfitting of the training dataset may occur during the training of the ML models. Hence, we currently support the use of both ML techniques and linear formulas to predict postoperative ACSs to obtain better-generalized results. We believe that the ML technique outperforms the traditional LR when additional measurements are added to a multimodal approach.

We did not build a binary classification model, such as logistic regression or random forest classifier, to predict low postoperative ACAs. There was a high risk of overfitting in the binary classification because

of the small number of patients with ACAs <20 degrees. Because the prediction models were trained using continuous values of postoperative ACAs, focusing on fitting all samples in the whole range and not on the boundary of ACAs <20 degrees, the binary classification performance was unsatisfactory. Further studies targeting the prediction of low postoperative ACAs are needed using more clinical data for accurate prediction.

A strength of this study was the collection of a large postoperative AS-OCT dataset for ACA prediction model development. In previous studies on postoperative ACA,[8,23] selection bias may have occurred because <100 samples were used for analysis. Our models used full preoperative biometric variables via LR or ML models compared with that of Nishida's model.[9] Using a larger dataset, we were able to develop ACA prediction models and validate them in the external dataset. Additionally, we attempted to maximize the predictive ability using ML techniques.

However, this study had several limitations. First, it had a retrospective design. Because the prediction model can support clinicians' choice of ICL size, prospective intervention studies are required to confirm the effectiveness of the proposed model. Second, the dataset consisted of an East Asian (South Korean) population from a single refractive surgery center. One study showed that structural biometrics measured using AS-OCT varied by ethnicity.[31] Generally, eyes in East Asians have smaller anterior segments than those in Caucasians. Therefore, we did not use a large lens (13.7 mm). Finally, ACA prediction models were developed using pre-operative AS-OCT measurements under dark conditions, without strict light control. The lighting condition can significantly affect the pupil diameter, iris thickness, and ACA.[32]

Conclusion

We developed models to comprehensively predict postoperative ACAs using pre-operative AS-OCT biometrics comprehensively showed that pre-operative data could potentially be used as good predictors of postoperative ACA narrowing. Furthermore, this method will facilitate the evaluation of postoperative ACA to prevent clinicians from overlooking the risks associated with ACA narrowing during the pre-operative assessment. Our ACA prediction algorithm is necessary for more accurate surgery with optimal ICL size selection.

Acknowledgments

References

1. Shimizu K, Kamiya K, Igarashi A, Shiratani T. Early clinical outcomes of implantation of posterior chamber phakic intraocular lens with a central hole (Hole ICL) for moderate to high myopia. *Br J Ophthalmol*. 2012;96(3):409–412.

2. Chen X, Wang X, Xu Y, et al. Five-year outcomes of EVO implantable collamer lens implantation for the correction of high myopia and super high myopia. *Eye Vis*. 2021;8(1):40.

3. Fernandes P, González-Méijome JM, Madrid-Costa D, Ferrer-Blasco T, Jorge J, Montés-Micó R. Implantable collamer posterior chamber intraocular lenses: a review of potential complications. *J Refract Surg*. 2011;27(10):765–776.

4. Yang W, Zhao J, Sun L, et al. Four-year observation of the changes in corneal endothelium cell density and correlated factors after Implantable Collamer Lens V4c implantation. *Br J Ophthalmol*. 2021;105(5):625–630.

5. Eissa SA, Sadek SH, El-Deeb MWA. Anterior Chamber Angle Evaluation following Phakic Posterior Chamber Collamer Lens with CentraFLOW and Its Correlation with ICL Vault and Intraocular Pressure. *J Ophthalmol*. 2016;2016:1383289.

6. Kang EM, Ryu IH, Lee G, et al. Development of a Web-Based Ensemble Machine Learning Application to Select the Optimal Size of Posterior Chamber Phakic Intraocular Lens. *Trans Vis Sci Tech*. 2021;10(6):5.

7. Kamiya K, Ryu IH, Yoo TK, et al. Prediction of Phakic Intraocular Lens Vault Using Machine Learning of Anterior Segment Optical Coherence Tomography Metrics. *Am J Ophthalmol*. 2021;226:90–99.

8. Fernández-Vigo JI, Macarro-Merino A, Fernández-Vigo C, et al. Effects of Implantable Collamer Lens V4c Placement on Iridocorneal Angle Measurements by Fourier-Domain Optical Coherence Tomography. *Am J Ophthalmol*. 2016;162:43–52.e1.

9. Nishida T, Kojima T, Kataoka T, Isogai N, Yoshida Y, Nakamura T. Prediction of the trabecular iris angle after posterior chamber phakic intraocular lens implantation. *J Cataract Refract Surg*. 2022;48(5):604–610.

10. Packer M. Meta-analysis and review: effectiveness, safety, and central port design of the intraocular collamer lens. *Clin Ophthalmol*. 2016;10:1059–1077.

11. Yoo TK, Ryu IH, Lee G, et al. Adopting machine learning to automatically identify candidate patients for corneal refractive surgery. *NPJ Digital Medicine*. 2019;2(1):59.

12. Igarashi A, Shimizu K, Kato S. Assessment of the Vault After Implantable Collamer Lens Implantation Using the KS Formula. *J Refractive Surg*. 2021;37(9):636–641.

13. Saito A, Kamiya K, Fujimura F, Takahashi M, Shoji N. Comparison of angle-to-angle distance using three devices in normal eyes. *Eye*. 2020;34(6):1116–1120.

14. Oh E, Yoo TK, Park EC. Diabetic retinopathy risk prediction for fundus examination using sparse learning: a cross-sectional study. *BMC Med Inform Decis Mak*. 2013;13:106.

15. Chang CC, Lin CJ. LIBSVM: A library for support vector machines. *ACM Trans Intell Syst Technol*. 2011;2(3):27:1–27:27.

16. Breiman L. Random forests. *Machine Learning*. 2001;45(1):5–32.

17. Chen C, Zhang Q, Yu B, et al. Improving protein-protein interactions prediction accuracy using XGBoost feature selection and stacked

ensemble classifier. *Computers in Biol and Med*. 2020;123:103899.

18. Deng YH, Luo XQ, Yan P, Zhang NY, Liu Y, Duan SB. Outcome prediction for acute kidney injury among hospitalized children via eXtreme Gradient Boosting algorithm. *Sci Rep*. 2022;12(1):8956.

19. Lundberg SM, Nair B, Vavilala MS, et al. Explainable machine-learning predictions for the prevention of hypoxaemia during surgery. *Nature Biomed Eng*. 2018;2(10):749.

20. Yoo TK, Ryu IH, Choi H, et al. Explainable Machine Learning Approach as a Tool to Understand Factors Used to Select the Refractive Surgery Technique on the Expert Level. *Transl Vis Sci Technol*. 2020;9(2):1–8.

21. shuang Ying G, MG Maguire, Glynn R, Rosner B. Tutorial on Biostatistics: Linear Regression Analysis of Continuous Correlated Eye Data. *Ophthalmic Epidemiology*. 2017;24(2):130–140.

22. Ying GS, Maguire MG, Glynn R, Rosner B. Tutorial on Biostatistics: Statistical Analysis for Correlated Binary Eye Data. *Ophthalmic Epidemiol*. 2018;25(1):1–12.

23. Singh R, Vanathi M, Kishore A, Tandon R, Singh D. An anterior segment optical coherence tomography study of the anterior chamber angle after implantable collamer lens-V4c implantation in Asian Indian Eyes. *Indian J Ophthalmol*. 2020;68(7):1418–1423.

24. Liu F, Xia F, Niu L, Zhao J, Wang X, Zhou X. Early Assessment of Circumferential Anterior Segment Structures Following Implantable Collamer Lens V4c Implantation Via SS-OCT. *Transl Vis Sci Technol*. 2022;11(11):4.

25. Niu L, Miao H, Han T, Ding L, Wang X, Zhou X. Visual outcomes of Visian ICL implantation for high myopia in patients with shallow anterior chamber depth. *BMC Ophthalmology*. 2019;19(1):121.

26. Chung TY, Park SC, Lee MO, Ahn K, Chung ES. Changes in iridocorneal angle structure and trabecular pigmentation with STAAR implantable collamer lens during 2 years. *J Refract Surg*. 2009;25(3):251–258.

27. Matarazzo F, Day AC, Fernandez-Vega Cueto L, Maurino V. Vertical implantable collamer lens (ICL) rotation for the management of high vault due to lens oversizing. *Int Ophthalmol*. 2018;38(6):2689–2692.

28. Yu AC, Mohajer B, Eng J. External Validation of Deep Learning Algorithms for Radiologic Diagnosis: A Systematic Review. *Radiology: Artificial Intelligence*. 2022;4(3):e210064.

29. Vaulet T, Al-Memar M, Fourie H, et al. Gradient Boosted Trees With Individual Explanations: An Alternative to Logistic Regression for Viability Prediction in the First Trimester of Pregnancy. *Computer Methods and Programs in Biomed*. 2022;213:106520.

30. Igarashi A, Shimizu K, Kato S, Kamiya K. Predictability of the vault after posterior chamber phakic intraocular lens implantation using anterior segment optical coherence tomography. *J Cataract Refract Surg*. 2019;45(8):1099–1104.

31. Qin B, Tang M, Li Y, Zhang X, Chu R, Huang D. Anterior Segment Dimensions in Asian and Caucasian Eyes Measured by Optical Coherence Tomography. *Ophthalmic Surg, Lasers and Imaging Retina*. 2012;43(2):135–142.

32. Hirose F, Hata M, Ito Shin-ichiro, Matsuki T, Kurimoto Y. Light–dark changes in iris thickness and anterior chamber angle width in eyes with occludable angles. *Graefes Arch Clin Exp Ophthalmol*. 2013;251(10):2395–2402.